IL NUOVO CIMENTO Vol. 34 C, N. 6 Novembre-Dicembre 2011
DOI 10.1393/ncc/i2011-11103-9

Colloquia: IFAE 2011

First results in heavy-flavor physics at CMS

R. Covarelli for the CMS Collaboration
University of Rochester - New York, NY, USA

(ricevuto il 29 Luglio 2011; pubblicato online il 21 Dicembre 2011)

Summary. — The analysis of data collected by the CMS experiment in 2010 (equivalent to an integrated luminosity of $40\,\mathrm{pb}^{-1}$) has yielded several physics results concerning the production mechanisms of heavy flavors at the unprecedented center-of-mass energy of 7 TeV. Recostruction techniques of heavy-flavored particles will be discussed, with particular focus on the triggers expressly designed to select them. Measurements of the $b\bar{b}$ cross-section both with jet "b-tagging" techniques and exclusive states, such as B^0, $B^{\pm}$ and B_s^0, will be presented, along with comparisons with theoretical predictions. Charmonium and bottomonium cross-section measurements, as well as the first determinations of the B-decay feed-down fraction for J/ψ, will be shown.

PACS 14.40.Pq – Heavy quarkonia.
PACS 14.65.Fy – Bottom quarks.

1. – Heavy-flavor physics at the CMS experiment

The CMS detector [1] at the LHC is a multi-purpose detector, mostly focused on direct searches for new particles: due to the versatility of the detector, especially of the High-Level Trigger (HLT) system, and to the excellent muon resolution down to low transverse momentum (p_T) values, however, interesting measurements in the field of heavy-flavor physics have been obtained. Results from the analysis of proton-proton data recorded in 2010 at a LHC center-of-mass energy of 7 TeV are presented.

1˙1. *The High-Level Trigger*. – The CMS HLT [2] runs on a farm of commercial CPUs on the events accepted by the Level-1 trigger decisions: it has full access to event data, allowing for precise object reconstruction and energy/momentum evaluation, by matching of information from different sub-detectors. At the lowest pp interaction rates, HLT for heavy-flavor physics is only based on single low-p_T muon objects and double-muon signals at Level 1. For higher luminosities, double-muon HLT and *ad hoc* solutions are adopted, where full reconstruction of both muons is not required, but particular states (*e.g.* the J/ψ meson) can be selected with loose cuts on the invariant mass of a HLT muon and a Level-1 muon, or a HLT muon and a charged track.

1˙2. *Offline muon reconstruction.* – In CMS muon candidates are defined as tracks reconstructed in the silicon tracker and associated to a compatible signal in the muon chambers. Two different muon types are available in CMS [3].

The first one (*Global Muons*) includes muons built as a combined fit to silicon and muon-chamber hits, belonging to independent tracks found in the tracker and muon systems. The second muon type (*Tracker Muons*) achieves a better reconstruction efficiency at lower momenta, at the expense of a slightly larger background: tracks found in the tracker and matched to only one muon segment are accepted and not refitted. Tracker muon identification is then provided by the angular matching between the two.

1˙3. *Muon efficiency determination.* – Muon trigger and reconstruction efficiencies are determined in CMS from the data using the "tag-and-probe" method, which uses well-known dimuon decays (the J/ψ, at low momenta) to provide a sample of "probe" objects. A well-identified muon, called "tag", is combined with a second object in the event and their invariant mass is computed. The tag-probe pairs are then divided into two samples, depending on whether the probe satisfies or not the criteria for the efficiency under consideration. The two tag-probe mass distributions contain a peak, the integral of which is the number of probes that satisfy or fail the criteria. The efficiency is extracted from a simultaneous unbinned maximum-likelihood fit to both mass distributions.

The statistical uncertainties in the muon efficiencies determined with the tag-and-probe method are used as a systematic uncertainty in the analyses. The hypothesis that the dimuon efficiency factorizes into the product of single-muon efficiencies is tested using Monte Carlo (MC) and corresponding systematic uncertainties are assigned.

2. – Quarkonium production cross-section

From the theoretical point of view, the prompt quarkonium cross-section is a clean probe of Non-Relativistic QCD approaches [4,5]. Charmonium is also interesting because, at relatively high p_T, a significant fraction of the J/ψ comes from b-hadron decays and, if it can be experimentally separated from the "prompt" component, provides a direct test of the Fixed-Order Next-to-Leading-Log (FONLL) prediction for the $b \to J/\psi$ production cross-section [6].

Inclusive charmonium and bottomonium events in CMS are reconstructed in the $Q\bar{Q} \to \mu^+\mu^-$ channel. Experimentally, the differential cross-sections can be expressed as

$$\frac{\mathrm{d}^2\sigma}{\mathrm{d}p_T\mathrm{d}y}(Q\bar{Q}) \cdot \mathrm{B}(Q\bar{Q} \to \mu^+\mu^+) = \frac{N_{\mathrm{rec}}(Q\bar{Q})}{\int \mathcal{L}\mathrm{d}t \cdot \langle A \cdot \varepsilon \rangle \Delta p_T \Delta y} \tag{1}$$

where $N_{\mathrm{rec}}(Q\bar{Q})$ is the $Q\bar{Q}$ yield in a given p_T-y bin, $\int \mathcal{L}\mathrm{d}t$ is the integrated luminosity, $\langle A \cdot \varepsilon \rangle$ is the average value of the geometrical acceptance (determined using MC simulation) times the reconstruction efficiency (from "tag-and-probe") of the dimuon, and $\Delta p_T \Delta y$ is the size of the bin. In the J/ψ case, multiplication by $1 - f_B$ (f_B) yields the prompt (non-prompt) component of the total inclusive cross-section.

The determination of inclusive cross-sections for J/ψ [7] and Υ [8] mesons is performed based on a similar strategy. Samples of 0.314 ± 0.035 $(3.1 \pm 0.3)\,\mathrm{pb}^{-1}$ data, are used for the J/ψ (Υ) analyses. Events are selected online by a double-muon trigger at Level 1. Muon tracks are then required to pass track-quality requirements. In the Υ analysis, a minimum muon p_T is also required, depending on the muon pseudo-rapidity. A dimuon candidate is accepted based on the χ^2 probability of the dimuon vertex fit.

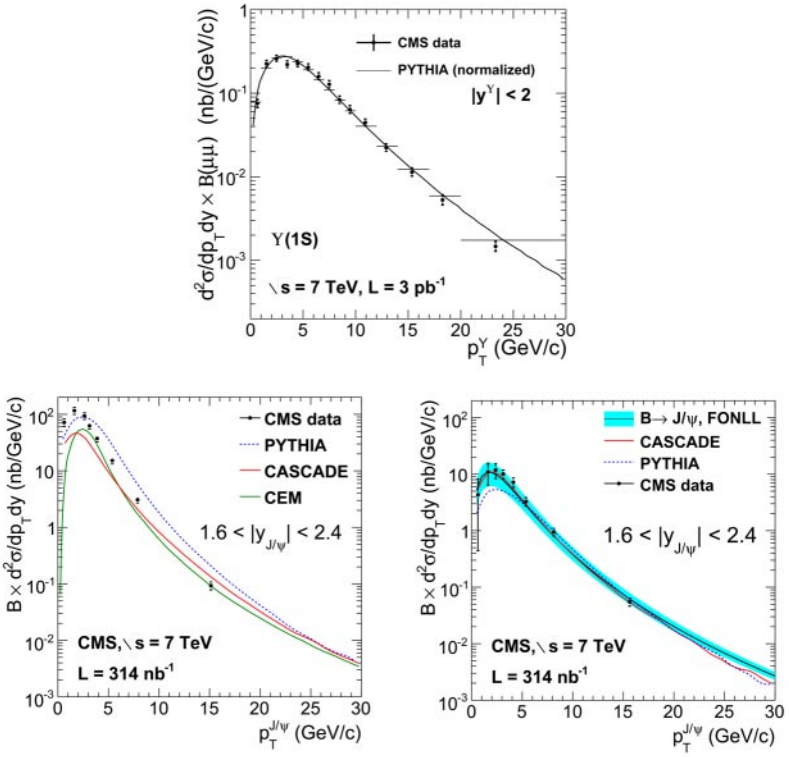

Fig. 1. – Measured differential cross-sections for Υ(1S) in the full rapidity region (top), prompt J/ψ (bottom left) and non-prompt J/ψ (bottom right) in the forward region, compared to theoretical calculations (black/colored lines).

Reconstructed yields are determined in bins of p_T-y using fits to the dimuon invariant mass distributions. In the Υ case, due to the presence of three partially overlapping states, some parameters are constrained to be the same for the three peaks. Empirical (exponential or polynomial) functions are used to model the backgrounds.

Differential cross-section results for the 3Υ states are derived as a function of p_T. Figure 1 top shows the Υ(1S) result compared to the PYTHIA prediction normalized to the data. The integrated cross-section in $|y| < 2.0$ is

$$B(\Upsilon(1\mathrm{S}) \to \mu^+\mu^-) \cdot \sigma(pp \to \Upsilon(1\mathrm{S}) + X) = 7.37 \pm 0.13(\mathrm{stat})^{+0.61}_{-0.42}(\mathrm{syst}) \pm 0.81(\mathrm{lumi})\mathrm{nb}\,.$$

In the J/ψ analysis, separation of prompt and non-prompt events is achieved using the distribution of the "pseudo-proper decay length" $\ell_{J/\psi} = L_{xy} \cdot m_{J/\psi}/p_T$, where $m_{J/\psi}$ is the J/ψ mass and L_{xy} is the most probable transverse decay length in the laboratory frame, computed from the positions of the primary and secondary vertex. To determine the fraction f_B of J/ψ from b-hadron decays, a simultaneous unbinned maximum-likelihood fit to the dimuon mass and the $\ell_{J/\psi}$ distribution is performed. The decay length of the prompt component are described by a simple resolution function, while a MC template parameterizing the longer lifetime of B decays is used for the non-prompt signal events.

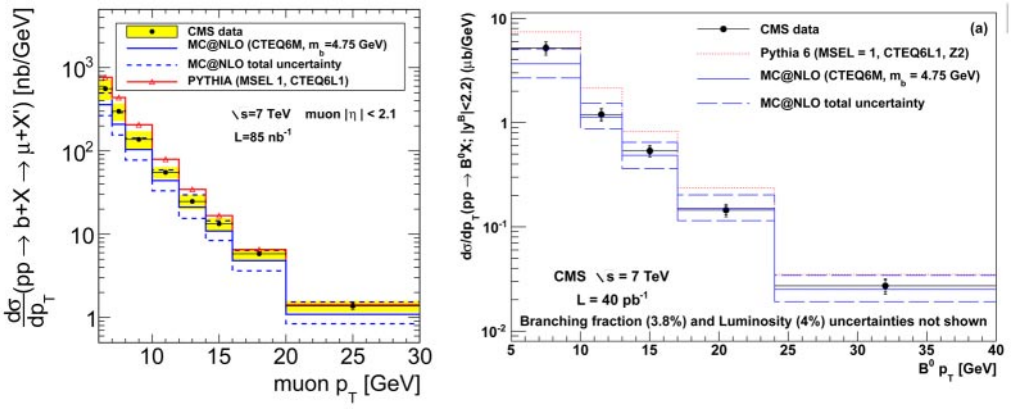

Fig. 2. – Measured differential cross-sections in p_T^μ for $b \to \mu$ (left) and in p_T^B for $B^0 \to J/\psi K_s^0$ (right), compared to MC-generator expectations (color histograms).

Differential cross-section results are derived for the prompt and non-prompt J/ψ for three different rapidity regions, using the B-fraction values. They are compared to theoretical and MC predictions (the FONLL prediction, the CASCADE generator [9], PYTHIA, and the color evaporation model (CEM) [10]) in fig. 1, bottom, showing a good agreement except for the low-p_T region of the prompt cross-section. Integration over p_T and rapidity gives, for the non-prompt cross-section in $6.5 < p_T < 30\,\mathrm{GeV}/c$, $|y| < 2.4$:

$$B(J/\psi \to \mu^+\mu^-) \cdot \sigma(pp \to b\bar{b} \to J/\psi + X) = 26.0 \pm 1.4(\mathrm{stat}) \pm 1.6(\mathrm{syst}) \pm 2.9(\mathrm{lumi})\mathrm{nb}\,.$$

3. – Inclusive $b \to \mu$ cross-section

Determinations of the $b\bar{b}$ cross-section have been performed with other methods than the $B \to J/\psi X$ analysis. The first one is based on the inclusive reconstruction of a semimuonic B decay, looking for a hadronic jet in the event and identifying it as a b-jet using the relative trasverse momentum (p_T^{rel}) of a reconstructed muon with respect to its thrust axis [11].

The study is based on an integrated luminosity of $85 \pm 9\,\mathrm{nb}^{-1}$. Events are selected by requiring a jet in the event with a "transverse energy" $E_T \equiv E \sin\theta > 1\,\mathrm{GeV}$ and a muon with $p_T > 3\,\mathrm{GeV}/c$ in the HLT and $> 6\,\mathrm{GeV}/c$ in the offline reconstruction. Standard muon quality criteria are applied to the latter.

The fraction of genuine b-jets in the selected sample is determined with a fit to the p_T^{rel} distribution using MC template functions for b-jets and jets from other sources (c jets and light-quark/gluon jets). Results are then corrected for acceptance, determined with MC simulation, and muon efficiency. The most important systematic sources are the uncertainty on the template shapes an the amount of underlying event activity.

The resulting differential cross-section in muon p_T is shown in fig. 2 left, compared to PYTHIA and MC@NLO [12] predictions, demonstrating the better agreement with NLO approaches. The integrated cross-section is computed to be

$$\sigma(pp \to b + X \to \mu + X') = 1.32 \pm 0.01(\mathrm{stat}) \pm 0.30(\mathrm{syst}) \pm 0.15(\mathrm{lumi})\,\mu\mathrm{b}$$

in the region $p_T^\mu > 6\,\mathrm{GeV}/c$, $|\eta^\mu| < 2.1$.

4. – Exclusive B cross-sections

Finally, the $b\bar{b}$ cross-section has been measured using exclusive B decay modes with well-measured branching fractions, namely: $B^{\pm} \to J/\psi K^{\pm}$ [13], $B^0 \to J/\psi K^0_s$ [14], and $B^0_s \to J/\psi\phi$ [15]. Analyses are performed on data samples with an integrated luminosity varying from 5 to 40 pb^{-1}.

Online and offline selection of J/ψ decays is very similar to the one discussed in sect. **2**. J/ψ candidates are then combined respectively to: a single charged track with $p_T > 900\,\mathrm{MeV}/c$; two tracks with an invariant mass compatible with that of the K^0_s, which form a common vertex having a transverse displacement significance $l_{xy}/\sigma(l_{xy}) > 5$; two tracks with an invariant mass tightly compatible with that of the ϕ resonance. Additional signal-to-background rejection comes from the χ^2 probability of vertices determined with all selected tracks (except those forming K^0_s candidates) and from fitting the invariant mass and the proper decay length at the same time, to account for prompt J/ψ background.

In all these analyses, the most important systematic contributions are tracking efficiency uncertainties and luminosity. As an example, the resulting differential cross-section in p_T^B for $B^0 \to J/\psi K^0_s$ is shown in fig. 2 right, compared to PYTHIA and MC@NLO predictions, confirming the good agreement observed with independent measurements in the latter case.

REFERENCES

[1] Chatrchyan S. *et al.* (The CMS Collaboration), *JINST*, **3** (2008) S08004.
[2] The CMS Collaboration, *CMS High Level Trigger*, CERN/LHCC 2007-021 (2007).
[3] The CMS Collaboration, *Performance of muon identification in pp collisions at* $\sqrt{s} =$ 7 *TeV*, CMS-PAS MUO-10-002 (2010).
[4] Lansberg J. -P., *Int. J. Mod. Phys. A*, **21** (2006) 3857.
[5] Bodwin G. T., Braaten E. and Lepage G. P., *Phys. Rev. D*, **51** (1995) 1125.
[6] Cacciari M., Greco M. and Nason P., *JHEP*, **9805** (1998) 007; Cacciari M. *et al.*, *JHEP*, **0407** (2004) 033.
[7] Khachatryan V. *et al.* (The CMS Collaboration), *Eur. Phys. J. C*, **71** (2011) 1575.
[8] Khachatryan V. *et al.* (The CMS Collaboration), *Phys. Rev. D*, **83** (2011) 112004.
[9] Jung H., *Comp. Phys. Commun.*, **143** (2002) 100.
[10] Halzen F., *Phys. Lett. B*, **69** (1977) 105; Fritzsch H., *Phys. Lett. B*, **67** (1977) 217; Gluck M., Owens J. F. and Reya E., *Phys. Rev. D*, **17** (1978) 2324; Barger V. D., Keung W. -J. and Phillips R. J. N., *Phys. Lett. B*, **91** (1980) 253.
[11] Khachatryan V. *et al.* (The CMS Collaboration), *JHEP*, **03** (2011) 090.
[12] Frixione S. and Webber B. R., *JHEP*, **06** (2002) 029; Frixione S., Nason P. and Webber B. R., *JHEP*, **08** (2003) 007.
[13] Khachatryan V. *et al.* (The CMS Collaboration), *Phys. Rev. Lett.*, **106** (2011) 112001.
[14] Khachatryan V. *et al.* (The CMS Collaboration), *Phys. Rev. Lett.*, **106** (2011) 252001.
[15] Khachatryan V. *et al.* (The CMS Collaboration), *Phys. Rev. D*, **84** (2011) 052008.